Pramana – J. Phys. (2022) 96:90
https://doi.org/10.1007/s12043-022-02327-w

Thermal phenomenon of Joule heating in the radiative flow of Carreau nanofluid

MUHAMMAD IRFAN[1],*, AAMIR NADEEM[1], NADEEM NASIR[1], MUHAMMD WAQAS[2] and WAQAR AZEEM KHAN[3,4]

[1]Department of Mathematical Sciences Federal Urdu University of Arts, Sciences & Technology , Islamabad 44000, Pakistan
[2]NUTECH School of Applied Sciences and Humanities, National University of Technology , Islamabad 44000, Pakistan
[3]Department of Mathematics, Faculty of Science, King AbdulAziz University, Jeddah 21589, Saudi Arabia
[4]Department of Mathematics, Mohi-ud-Din Islamic University, Nerian Sharif 12010, Pakistan
*Corresponding author. E-mail: mirfan@math.qau.edu.pk

MS received 15 July 2020; revised 14 October 2021; accepted 5 December 2021

Abstract. Recently, nanotechnology, especially the phenomena affecting the properties of flow and heat transport of nanofluid, has attracted considerable attention of researchers. In this study, the influence of Joule heating and chemical reaction in magnetite Carreau nanofluid has been elaborated considering the properties of radiation and convective phenomena. Additionally, the variable wall temperature and wall concentration have been reported. The bvp4c algorithm has been considered for solution progression. The influential variables are depicted graphically. The result reports that the temperature field increases for Eckert and magnetic numbers. The other output increases the concentration field for chemical reaction factor and decays for Brownian factor. Furthermore, comparison tables are given to show that our results agree with the results from earlier studies.

Keywords. Carreau nanofluid; Joule heating; thermal radiation; chemical reaction; variable characteristics.

PACS Nos **44.40.+a; 47.10.A-; 02.60.Cb; 47.55.pb**

1. Introduction

Magnetohydrodynamics (MHD) has widespread applications in engineering and industry, and fluids with MHD aspects have the ability to control flow separation, enhance heat transfer rate through the conducting fluids and manipulate the flow fields. Alfven first introduced the MHD. The MHD equations described here are the combinations of Maxwell equations on electromagnetic and fluid mechanics Navier–Stokes equations. With the MHD electric flow, the flow is induced with the magnetic field and described as a force in the momentum equation. The commonly used examples of MHD are power generators, MHD accelerators, crystal growth and the cooling of nuclear reactors. Krishna [1] studied the influence of ion slip and the Hall effect on the time-dependent MHD rotating flow of viscoelastic fluid. He showed that the velocity and temperature fields are always higher than the ramped wall temperature and in favour of isothermal plates. Khader and Sharma [2] analysed FDM simulations of time-dependent MHD non-Newtonian fluid flow with thermal radiation and heat source. Goud [3] demonstrated the effect of heat generation on steady MHD micropolar fluid flow through a permeable medium with variable injection. Selvaraj and Jothi [4] analysed the impact of heat sources on MHD fluid flow and showed that the flow is generated by the exponential movement of the vertical plate. Temperature and mass diffusion variations are also taken exponentially through the permeable medium. Irfan *et al* [5] discussed the modern theory of mass flux in MHD Carreau nanofluid with Arrhenius activation energy. The concentration field increases for activation energy and thermophoretic factors. Various researches in these directions are reported in refs [6–13].

Recently, nanotechnology has become an important area of science, and the phenomena affecting the flow and heat transport of nanofluids have attracted consid-

Published online: 28 April 2022

erable attention of researchers [14–20]. Ahmed *et al* [21] reported the concept of rotating disk in Maxwell nanofluid. The increase in radiation and thermophoresis factors increases the fluid temperature. Irfan [22] examined the variable properties in Carreau nanfluid by considering nanoparticles. He noted that destructive and constructive reaction factors have opposite influences on the concentration field. Li *et al* [23] explored nanofluid applications and research. Rafiq *et al* [24] presented the activation energy aspects in radiated Maxwell nanofluids. They showed that temperature and concentration scatterings have conflicting impacts for Brownian factors.

This study examines the Joule heating properties and chemical reactions in magnetite Carreau nanofluid. Thermal aspects of convective conditions and radiation are also studied. The bvp4c algorithm executed the solution process. The influential factors are studied.

2. Development of the model

We analyse the transient flow of 3D radiative Carreau nanofluid considering the aspects of Joule heating with stretching velocities

$$U_w = \frac{ax}{1-\beta t} \quad \text{and} \quad V_w = \frac{by}{1-\beta t},$$

respectively, perpendicular to x- and y-directions. The magnetic strength (B_0) is applied parallel to the z-axis. Moreover, a chemical reaction is examined. Hence, the Carreau nanofluid flow equations are reported as follows:

$$\frac{\partial u}{\partial x} + \frac{\partial v}{\partial y} + \frac{\partial w}{\partial z} = 0, \tag{1}$$

$$u\frac{\partial u}{\partial x} + v\frac{\partial u}{\partial y} + w\frac{\partial u}{\partial z} = \frac{\partial u}{\partial t} - \nu\left(\frac{\partial^2 u}{\partial z^2}\right)\left\{\left[1+\left(\Gamma\frac{\partial u}{\partial z}\right)^2\right]^{\frac{n-1}{2}} + (n-1)\left(\Gamma\frac{\partial u}{\partial z}\right)^2\left[1+\left(\Gamma\frac{\partial u}{\partial z}\right)^2\right]^{\frac{n-3}{2}}\right\} - \frac{\sigma B^2(t)u}{\rho}, \tag{2}$$

$$u\frac{\partial v}{\partial x} + v\frac{\partial v}{\partial y} + w\frac{\partial v}{\partial z} = \frac{\partial v}{\partial t} - \nu\left(\frac{\partial^2 v}{\partial z^2}\right)\left\{\left[1+\left(\Gamma\frac{\partial v}{\partial z}\right)^2\right]^{\frac{n-1}{2}} + (n-1)\left(\Gamma\frac{\partial v}{\partial z}\right)^2\left[1+\left(\Gamma\frac{\partial v}{\partial z}\right)^2\right]^{\frac{n-3}{2}}\right\} - \frac{\sigma B^2(t)v}{\rho}, \tag{3}$$

$$u\frac{\partial T}{\partial x} + v\frac{\partial T}{\partial y} + w\frac{\partial T}{\partial z} = \frac{\partial T}{\partial t} - \alpha\frac{\partial^2 T}{\partial z^2} + \tau\left[\left(\frac{D_T}{T_\infty}\right)\left(\frac{\partial T}{\partial z}\right)^2 + D_B\left(\frac{\partial C}{\partial z}\frac{\partial T}{\partial z}\right)\right] - \frac{1}{\rho c_p}\frac{\partial q_r}{\partial z} - \frac{\sigma B^2(t)}{\rho c_p}(u^2+v^2), \tag{4}$$

$$u\frac{\partial C}{\partial x} + v\frac{\partial C}{\partial y} + w\frac{\partial C}{\partial z} = \frac{\partial C}{\partial t} - D_B\left(\frac{\partial^2 C}{\partial z^2}\right) + \frac{D_T}{T_\infty}\left(\frac{\partial^2 T}{\partial z^2}\right) - k_c(C-C_\infty)^m, \tag{5}$$

$$U_w = u = \left(\frac{ax}{1-\beta t}\right), \quad V_w = v = \left(\frac{by}{1-\beta t}\right),$$

$$w = 0, \quad -k\frac{\partial T}{\partial z} = h_f(T_w - T),$$

$$C = C_w(x,\, t) \quad \text{at} \quad z = 0, \tag{6}$$

$$u \to 0, \quad v \to 0, \quad T \to T_\infty,$$

$$C \to C_\infty \quad \text{as} \quad z \to \infty. \tag{7}$$

Here $(x,\ y,\ z)$ are velocity components along (u, v, w)-directions. Furthermore, $(\nu, \Gamma, n, \sigma, B_0, \rho, T, C, c_p,\ \tau, D_B, D_T, T_\infty, C_\infty, k_c)$ are the kinematic viscosity, material rate constant, power-law index, electrical conductivity, magnetic constant, fluid density, temperature, concentration, heat capacity, effective heat capacity ratio, Brownian diffusion coefficient, thermophoresis diffusion coefficient, nanofluid ambient temperature, nanofluid ambient concentration, reaction rate factor, respectively.

The magnetic field $B(T)$, wall temperature $T_w(x,\ t)$, wall concentration $C_w(x,\ t)$ and radiative heat flux q_r are given as

$$B(T) = \frac{B_0}{\sqrt{1-\beta t}},$$

$$T_w(x,\ t) = \frac{T_0 a x^2}{\nu\,(1-\beta t)^{\frac{3}{2}}} + T_\infty,$$

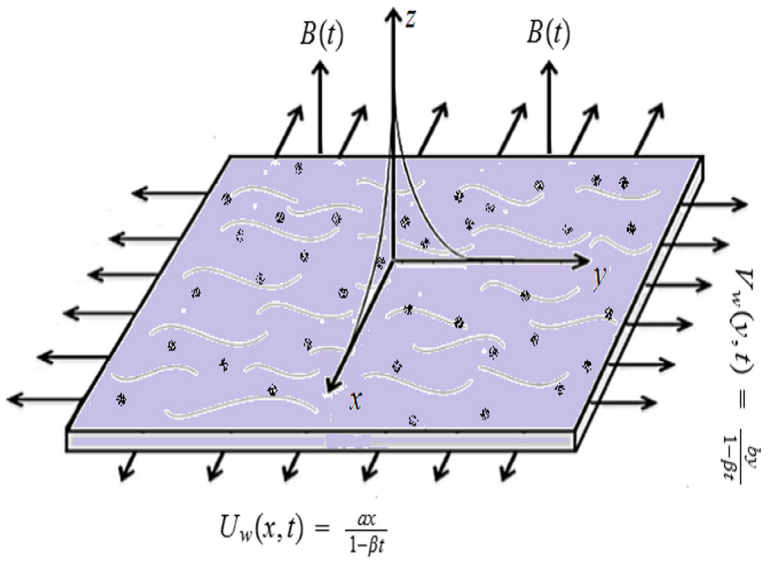

Figure 1. Schematic diagram.

$$C_w(x,\ t) = \frac{C_0 a x^2}{\nu\,(1-\beta t)^{\frac{3}{2}}} + C_\infty,$$
$$q_r = \frac{-16\sigma^* T_\infty^3}{k^*}\frac{\partial T}{\partial z}. \tag{8}$$

where T_0, C_0 are the reference temperature and concentration, respectively.

2.1 *Appropriate conversions*

Consider

$$u = f'(\eta)\left(\frac{ax}{1-\beta t}\right), \quad v = g'(\eta)\left(\frac{ay}{1-\beta t}\right),$$
$$w = -[f(\eta)+g(\eta)]\sqrt{\frac{a\nu}{1-\beta t}},$$
$$\theta\,(\eta) = \frac{T-T_\infty}{T_w-T_\infty}, \quad \phi = \frac{C-C_\infty}{C_w-C_\infty}$$
$$\eta = \sqrt{\frac{a}{\nu\,(1-\beta t)}}z. \tag{9}$$

Equations (9) with (8) reduce eqs (1)–(7) into

$$[1+nWe_1^2 f''^2][1+We_1^2 f''^2]^{\frac{n-3}{2}} f''' - f'^2 + ff'' + gf'' - Sf' - \frac{1}{2}\eta S f'' + M^2 f' = 0, \tag{10}$$

$$[1+nWe_2^2 g''^2][1+We_2^2 g''^2]^{\frac{n-3}{2}} g''' - g'^2 + fg'' + gg'' - Sg' - \frac{1}{2}\eta S g'' + M^2 g' = 0, \tag{11}$$

$$\theta'' + \frac{4}{3}R\theta'' + \Pr\, f\theta' + \Pr\, g\theta' - \Pr\frac{S}{2}\left(3\theta+\eta\theta'\right) + \Pr\, N_T\theta'^2 + \Pr\, N_B\theta'\phi' - 2\Pr\, f'\theta + M^2\, Ec(f'^2+g'^2) = 0, \tag{12}$$

$$\phi'' + Le\Pr\, f\phi' + Le\Pr\, g\phi' - 2\,Le\Pr\, f'\phi' - \Pr\, Le\frac{S}{2}\left(3\phi+\eta\phi'\right) + \left(\frac{N_T}{N_B}\right)\theta'' - Le\Pr\, C_R\phi^m = 0, \tag{13}$$

$$f(0)=0, \quad g(0)=0, \quad f'(0)=1, \quad g'(0)=\alpha,$$
$$\theta'(0)+\gamma_t\theta(0) = -\gamma_t, \quad \phi(0)=0, \tag{14}$$
$$f'\to 0, \quad g'\to 0, \quad \theta\to 0,$$
$$\phi\to 0 \ \text{ as } \ \eta\to\infty. \tag{15}$$

Here (We_1, We_2, S, M, α, γ_t, R, N_B, N_T, E_c, Pr, Le, C_R) signify the local Weissenberg numbers, unsteadiness, magnetic, ratio of stretching rates, thermal Biot radiation, Brownian motion, thermophoresis, respectively, whereas Ec is the Eckert number, Pr is the Prandtl number, Le is the Lewis number, C_R is chemical reaction factor. These expressions are given as

$$(We_1,\ We_2) = \left(\sqrt{\frac{\Gamma^2 a^3 x^2}{\nu(1-\beta t)^2}}, \sqrt{\frac{\Gamma^2 a^3 y^2}{\nu(1-\beta t)^2}}\right),$$
$$S = \frac{\beta}{a}, \quad M = \sqrt{\frac{\sigma B_0^2(1-\beta t)}{\rho_f a}},$$
$$\alpha = \frac{b}{a}, \quad R = \frac{4\sigma^* T_\infty^3}{kk^*}, \quad N_B = \frac{\tau D_B(C_w-C_\infty)}{\nu},$$
$$N_T = \frac{\tau D_T(T_w-T_\infty}{\nu T_\infty}, \quad Ec = \frac{U_w(x,t)}{c_p(T_w-T_\infty)},$$

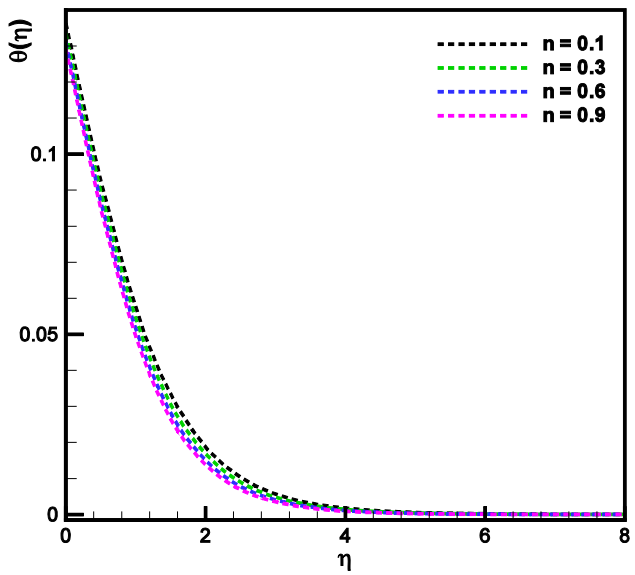

Figure 2. Plot of η vs. $\theta(\eta)$ for $n < 1$.

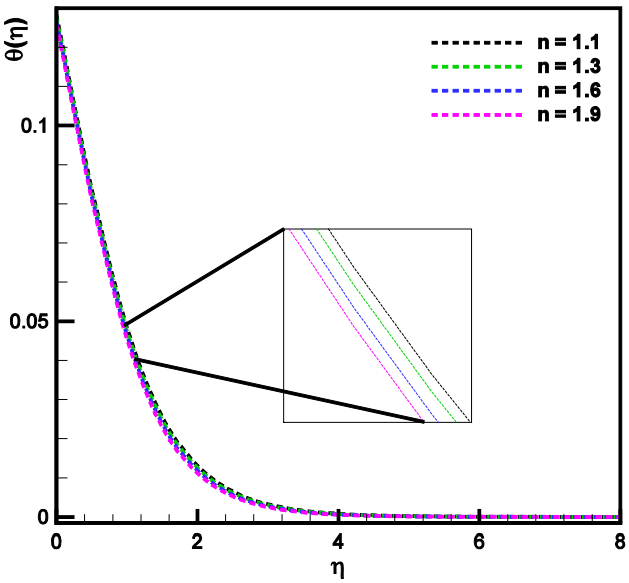

Figure 3. Plot of η vs. $\theta(\eta)$ for $n > 1$.

$$\mathrm{Pr} = \frac{\nu}{\alpha_1}, \quad Le = \frac{\alpha_1}{D_B}, \quad \gamma_t = \frac{h_f}{k}\sqrt{\frac{\nu(1-\beta t)}{a}},$$
$$C_R = \frac{k_c(1-\beta t)^2}{a}. \tag{16}$$

3. Physical quantities

Here the expressions of skin friction coefficients (C_{fx}, C_{fy}), Nusselt numberNu_x and Sherwood number Sh_x are

$$C_{fx} = \frac{\tau_{xz}}{\frac{1}{2}\rho_f U_w^2} \quad \text{and} \quad C_{fy} = \frac{\tau_{yz}}{\frac{1}{2}\rho_f U_w^2}, \tag{17}$$
$$Nu_x = \left(-\frac{x}{(T_w - T_\infty)} + \frac{xq_r}{k\,(T_w - T_\infty)}\right)\left.\frac{\partial T}{\partial z}\right|_{z=0},$$
$$Sh_x = -\frac{x\left.\frac{\partial C}{\partial z}\right|_{z=0}}{(C_w - C_\infty)}. \tag{18}$$

The dimensionless variables are

$$\frac{1}{2}C_{fx}Re_x^{\frac{1}{2}} = [1 + We_1^2 f''^2(0)]^{\frac{n-1}{2}} f''(0),$$
$$\frac{1}{2}\left(\frac{U_w}{V_w}\right)C_{fy}Re_x^{\frac{1}{2}} = [1 + We_2^2 g''^2(0)]^{\frac{n-1}{2}} g''(0), \tag{19}$$
$$Re_x^{-\frac{1}{2}}Nu_x = -\left(1 + \frac{4}{3}R\right)\theta'(0),$$
$$Re_x^{-\frac{1}{2}}Sh_x = -\phi'(0), \tag{20}$$

where $Re_x = \frac{ax^2}{\nu(1-\beta t)}$ signifies the local Reynolds number.

4. Analysis of results

This section, using numerical bvp4c algorithm, discloses the tabular outcomes and graphical illustration of radiative 3D Carreau nanofluid fluid flow with Joule heating. Furthermore, various fixed values of significant parameters $S = C_R = 0.1$, $M = N_T = \gamma_t = 0.2$, $R = N_B = 0.3$, $A = Ec = 0.5$, $n = 0.6$, $m = 2$, $Le = 1.0$, $\mathrm{Pr} = 1.2$ and $We_1 = We_2 = 1.5$ are considered excepting specific values in graphs.

Figures 2 and 3 present the influence of power-law exponent (n); $n < 1$ for shear-thinning liquid and $n > 1$ for shear-thickening liquid. These plots show that for both circumstances the temperature of Carreau fluid declines. For $n < 1$, the temperature field decreases. Similar behaviour has been reported for $n > 1$.

Figures 4 and 5 present the influence of Eckert number (Ec) and Brownian motion factor (N_B) on the temperature field. The larger Ec enhances the temperature field. Physically, due to friction, the heat energy is stored in the fluid, and the mechanical energy is converted into thermal energy. Therefore, the temperature of the Carreau liquid is higher. Similar performance has been detected for N_B. The random movement of atoms grow which intensifies the temperature of the Carreau nanofluid.

Figures 6 and 7 present the influence of magnetic factor (M) and Prandtl number (Pr) on the temperature field. The increasing values of M increase the temperature field; however, the opposite is reported for Pr. When M increases, the Lorentz force increases, because the Lorentz force imparts extra heat to the fluid which inflates the temperature field. The contradictory impact has been seen for Pr.

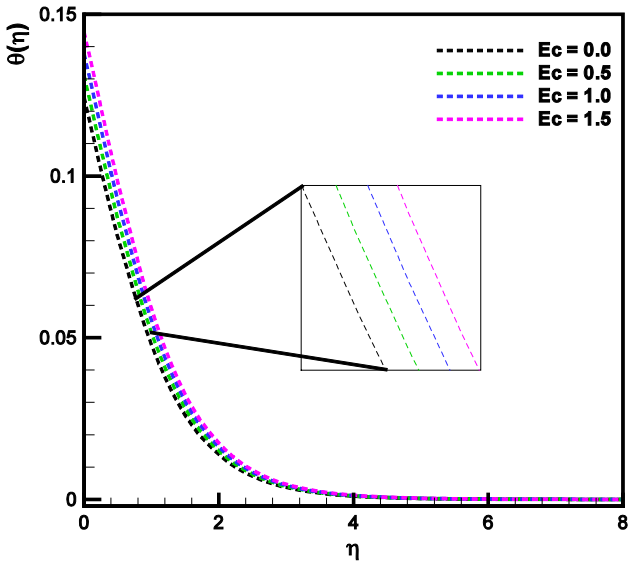

Figure 4. Plot of η vs. $\theta(\eta)$ for various values of Ec.

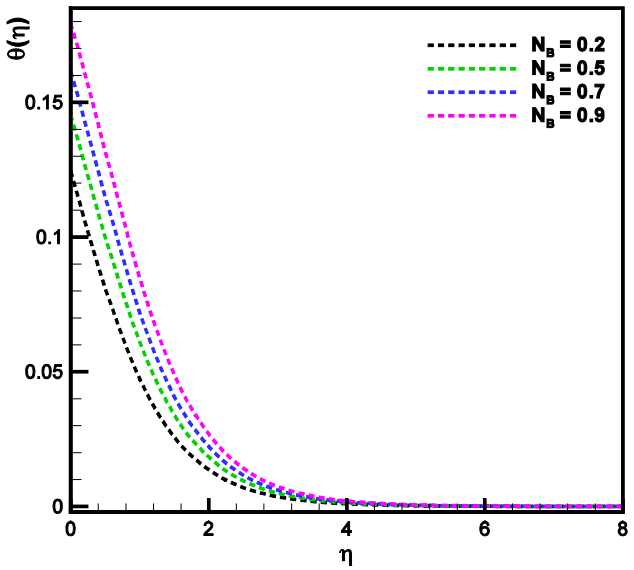

Figure 5. Plot of η vs. $\theta(\eta)$ for various values of N_B.

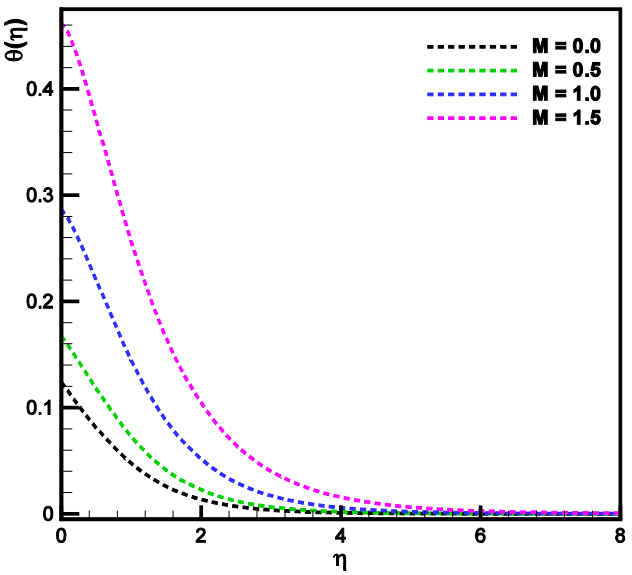

Figure 6. Plot of η vs. $\theta(\eta)$ for various values of M.

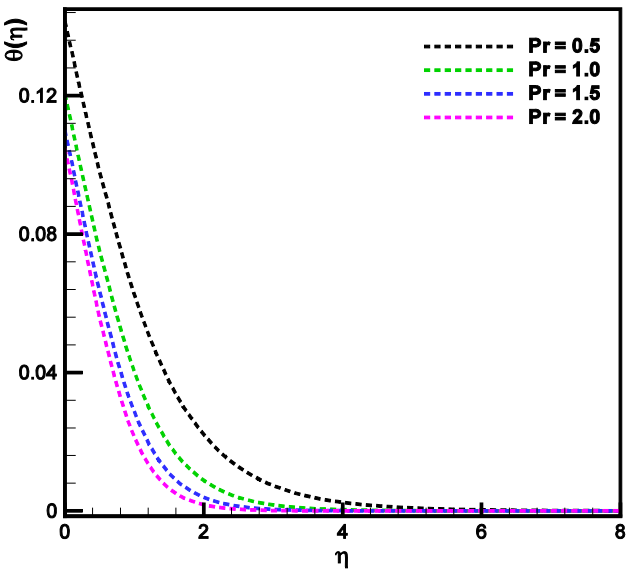

Figure 7. Plot of η vs. $\theta(\eta)$ for various values of Pr.

Figures 8 and 9 present the influence of Brownian motion (N_B) and thermophoresis (N_T) factors on the concentration field. The concentration field decreases for N_B and increases for N_T when N_B and N_T increase. For higher N_B the particle collision grows which declines the concentration field. Furthermore, the transportation of the nanoparticles is arises from the superior area to the inferior area which increases the concentration field.

Figures 10 and 11 show the influence of chemical reaction factor (C_R) and Lewis number (Le) on the concentration field. The larger C_R decays the concentration field. The quantity of generative chemical reactions is advanced for better which declines the concentration field. Moreover, the progressive assessment of Le reduces the coefficient of Brownian diffusion and decreases the concentration field.

Table 1 gives the comparison of $-f''(0)$ for S with earlier literature. This table illustrates remarkable outcomes with existing numerical outcomes. Table 2 shows the numerical results of $-\theta'(0)$ and $-\phi'(0)$ for Ec, N_B, N_T and γ_t for $n = 0.6$ and $n = 1.6$. The transport of heat decreases for N_B and N_T for $n = 0.6$ and $n = 1.6$; however, it increases for γ_t. The mass transport increases for N_B, while it decays for N_T and γ_t.

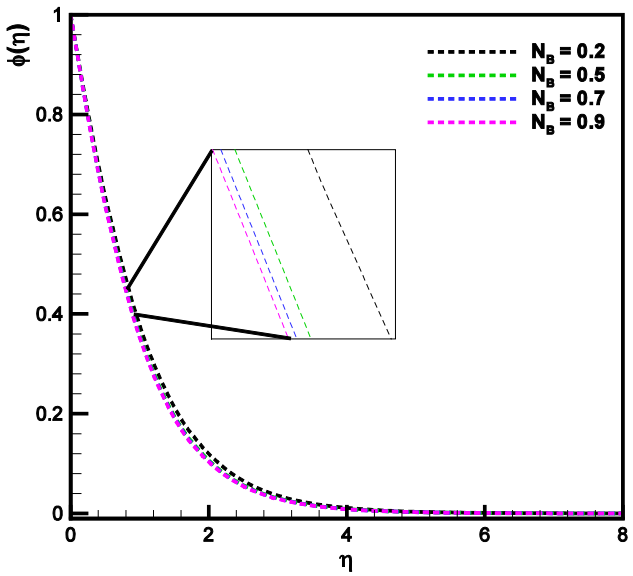

Figure 8. Plot of η vs. $\phi(\eta)$ for various values of N_B.

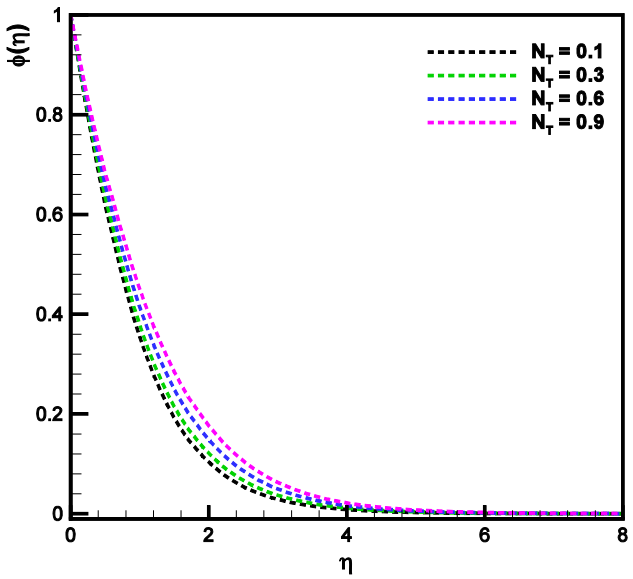

Figure 9. Plot of η vs. $\phi(\eta)$ for various values of N_T.

Furthermore, reverse performance can be seen for Ec for both $n = 0.6$ and $n = 1.6$ for $-\theta'(0)$ and $-\phi'(0)$.

5. Conclusions

Here the properties of higher-order chemical reaction in Carreau nanofluid elaborating the aspects of Joule heating and radiation have been disclosed numerically. Additionally, convective conditions and magnetic properties are examined. The achieved results are summarised as follows:

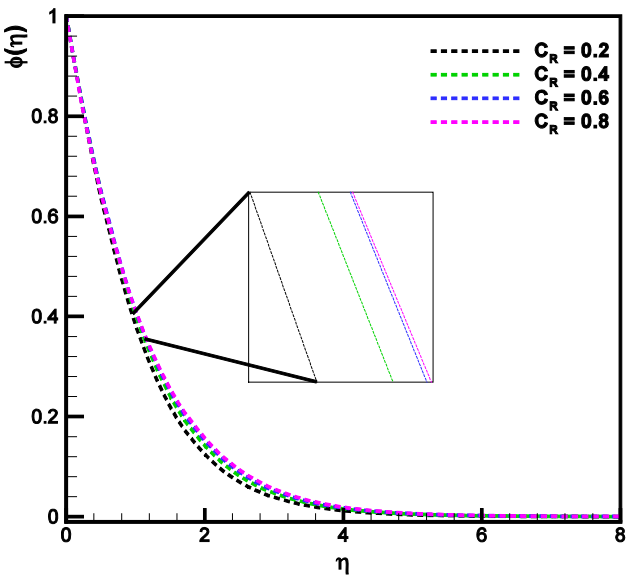

Figure 10. Plot of η vs. $\phi(\eta)$ for various values of C_R.

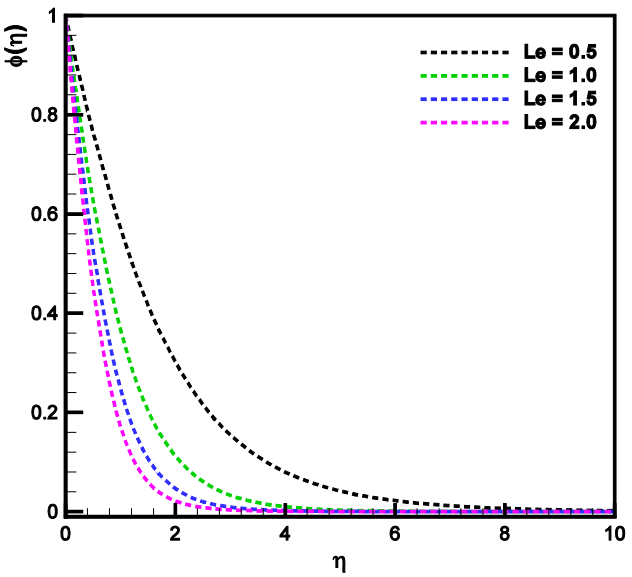

Figure 11. Plot of η vs. $\phi(\eta)$ for various values of Le.

- The Carreau fluid temperature increased for M and Ec.
- The power-law exponent n decreased the temperature field for $(n = 0.6)$ and $(n = 1.6)$.
- Contradictory influences can be seen for N_t and N_b on the concentration field.
- The concentration field increased for C_R.

Table 1. For the Newtonian case, the comparative outcomes of $-f''(0)$ for S.

	$-f''(0)$		
S	Sharidan *et al* [25]	Chamkha *et al* [26]	Present (bvp4c)
0.8	1.2610420	1.2615120	1.2610426
1.2	1.3777220	1.3780520	1.3777252
2.0	1.5873620	–	1.5873702

Table 2. Numerical outcomes of $-\theta'(0)$ when $S = C_R = 0.1$, $M = 0.2$, $R = 0.3$, $A = 0.5$, $n = 0.6$, $m = 2$, $Le = 1.0$, $\Pr = 1.2$ and $We_1 = We_2 = 1.5$ are fixed.

Ec	N_B	N_T	γ_t	$-\theta'(0)$		$-\phi'(0)$	
				$n = 0.6$	$n = 1.6$	$n = 0.6$	$n = 1.6$
0.5	0.3	0.2	0.2	0.108054	0.108548	0.788771	0.834730
0.6				0.107885	0.108740	0.789104	0.834348
0.7				0.107716	0.108932	0.789438	0.833967
0.8				0.107547	0.109124	0.789771	0.833586
0.5	0.4			0.106535	0.107631	0.806017	0.850525
	0.5			0.104943	0.106064	0.816596	0.860902
	0.6			0.103278	0.104423	0.823868	0.868021
	0.3	0.3		0.107858	0.108936	0.759021	0.804468
		0.4		0.107660	0.108745	0.729545	0.775624
		0.5		0.107459	0.108551	0.700348	0.747058
		0.2	0.1	0.0608341	0.061143	0.813723	0.858446
			0.3	0.145628	0.147641	0.769740	0.814372
			0.5	0.201417	0.205400	0.742903	0.786864

References

[1] M V Krishna, *Int. Commun. Heat Mass Transf.* **119**, 104927 (2020)
[2] M M Khader and R P Sharma, *Math. Comp. Simul.* **181**, 333 (2021)
[3] B S Goud, *Int. J. Thermofluids* **7–8**, 100044 (2020)
[4] Selvaraj and E Jothi, *Mater. Today: Proc.* **46**, 3490 (2021)
[5] M Irfan, K Rafiq, M Khan, M Waqas and M S Anwar, *Int. Commun. Heat Mass Transf.* **120**, 105051 (2021)
[6] P V S Narayana and D H Babu, *J. Taiwan Inst. Chem. Eng.* **59**, 18 (2016)
[7] M Waqas, M I Khan, T Hayat and A Alsaedi, *Comput. Meth. Appl. Mech. Eng.* **324**, 640 (2017)
[8] N Nithyadevi, P Gayathri and N Sandeep, *Int. J. Mech. Sci.* **131–132**, 827 (2017)
[9] S Muhammad, G Ali, S I A Shah, M Irfan, W A Khan, M Ali and F Sultan, *Pramana – J. Phys.* **93**, 40 (2019)
[10] N Tarakaramu, P V S Narayana and B Venkateswarlu, *Appl. Math. Sci. Comput.* 87 (2019)
[11] M Irfan and M Khan, *Appl. Nanosci.* **10**, 2977 (2019)
[12] T Thirupathi and P V S Narayana, *Austr. J. Mech. Eng.* 1 (2020)
[13] K K Naidu, D H Babu, S H Reddy and P V S Narayana, *J. Therm. Sci. Eng. Appl.* **13**, 031011 (2021)
[14] S U S Choi and J A Eastman, *ASME Int. Mech. Eng. Congr. Expo.* 99 (1995)
[15] R M Mostafizur, M H U Bhuiyan, R Saidur and A R Abdul-Aziz, *Int. J. Heat Mass Transf.* **76**, 350 (2014)
[16] P V S Narayana, B Venkateswarlu and S Venkataramana, *Heat Transf. Asian Res.* **44**, 1 (2015)
[17] P V S Narayana, *J. Nanofluids* **6**, 1181 (2017)
[18] B Mahanthesh, B J Gireesha and R S R Gorla, *J. Ass. Arab. Uni. Basic Appl. Sci.* **23**, 75 (2017)
[19] M Khan, M Irfan and W A Khan, *Pramana – J. Phys.* **92**, 17 (2019)
[20] M Irfan, K Rafiq, M S Anwar, M Khan, W A Khan and K Iqbal, *Pramana – J. Phys.* **95**, 1 (2021)
[21] J Ahmed, M Khan and L Ahmad, *Phys. Lett.* **383**, 1300 (2019)
[22] M Irfan, *Surf. Interfaces* **23**, 100926 (2021)
[23] J Li, X Zhang, B Xu and M Yuan, *Int. Commun. Heat Mass Transf.* **127**, 105543 (2021)
[24] K Rafiq, M Irfan, M Khan, M S Anwar and W A Khan, *Phys. Scr.* **94**, 045002 (2021)
[25] S Sharidan, T Mahmood and I Pop, *Int. J. Appl. Mech. Eng.* **11**, 647 (2006)
[26] A J Chamkha, A M Aly and M A Mansour, *Chem. Eng. Commun.* **197**, 846 (2010)